FIRST FACULTY
OF MEDICINE
Charles University

Self-report of a doctoral thesis: Neuronal coding and metabolic cost of information

Tomáš Bárta

2023

En cotutelle study program:

Biomedical informatics
at Charles University and Czech Academy of Sciences

Neuroscience
at Sorbonne University

Supervisors:

Lubomír Košťál
Laboratory of Computational Neuroscience
Institute of Physiology of the Czech Academy of Sciences

Philippe Lucas
Department of Sensory Ecology
Institute of Ecology and Environmental Sciences - Paris
National Research Institute for Agriculture, Food and the Environment

Contents

Abstract in English

For most neurons, the information the neuron passes on is contained within the times of sending out electrical pulses - so-called action potentials. It is still not fully understood how to read this „neural code“. The efficient coding hypothesis proposes that due to evolutionary pressures sensory systems evolved to transmit and process information in the most efficient way possible. However, the notion of efficiency seems to be different in different sensory systems. Cortical neurons keep their firing rates low to minimize metabolic expenses. So do insect olfactory receptor neurons (ORNs, the first layer of the olfactory system). Neurons in the insect antennal lobe (the second layer of the olfactory system), on the other hand fully use the space of possible firing rates to encode the maximum information about the odor. In my thesis, I studied how can single cortical neurons and their populations transmit and process information, while keeping metabolic expenses low, and also how the insect olfactory system encodes information about odors encountered in the air.

In the part of my thesis about metabolically efficient information transmission I focused mainly on the role of inhibitory neurons in efficient information transmission. Through mathematical analysis and Monte Carlo simulations of spiking neuronal models, I show how can the input from pre-synaptic inhibitory neurons decrease the trial-to-trial variability of the post-synaptic neuron, and by generalizing these results to a recurrent neural network I illustrated how the trial-to-trial variability can decrease with a stimulus-onset, phenomenon known as neural variability quenching. However, an information-theoretical analysis showed that the input from inhibitory neurons in the form of inhibitory feedback with a stimulus onset will only yield significant improvements in metabolically efficient information transmission if the information is being transmitted by a population of recurrently connected neurons, rather than a single neuron.

To understand the general principles governing neural coding, I next focused on the neural activity of the insect olfactory system. I analyzed the local field potentials (LFPs) and firing activity of insect ORNs stimulated with a novel odor-delivery device, capable of temporally

precise stimulus delivery. These novel recordings showed that moth ORNs are much more capable of encoding the stimulus duration than previously thought. The properties of moth ORNs were revealed to be very similar to the properties of the majority of Drosophila ORNs, which allows the unification of the research on those species. Using the recordings of the LFPs I constructed a minimal model of the moth ORN, which reliably describes the firing activity while using only several interpretable parameters.

A simple and transferable model, that can describe the firing activity of the ORNs is essential for building an integrative model of the insect olfactory system. Such a model could be used to study the information-metabolic efficiency of the whole system and analyze if under certain conditions the high firing rates in the antennal lobe actually aid the information-metabolic efficiency. Therefore, the results of my thesis are a step forward to understanding the general principles governing the neural code.

Abstrakt česky

U většiny neuronů je informace, kterou neuron předává, obsažena v časech vysílání elektrických impulzů - tzv. akčních potenciálů. Dosud není zcela jasné, jak tento "neuronový kód" číst. Hypotéza efektivního kódování předpokládá, že v důsledku evolučních tlaků se smyslové systémy vyvinuly tak, aby přenášely a zpracovávaly informace co nejefektivnějším způsobem. Zdá se však, že pojem efektivity se v různých smyslových systémech liší. Kortikální neurony udržují nízkou frekvenci vysílání akčních potentiálů, aby minimalizovaly metabolické náklady. Podobně to dělají i hmyzí čichové receptorové neurony (ORN, první vrstva čichového systému). Neurony v hmyzím tykadlovém laloku (druhá vrstva čichového systému) naopak plně využívají prostor možných frekvencí, aby zakódovaly maximum informací o pachu. Ve své diplomové práci jsem se zabýval tím, jak mohou jednotlivé korové neurony a jejich populace přenášet a zpracovávat informace při zachování nízkých metabolických nákladů a také tím, jak hmyzí čichový systém kóduje informace o paších, které se vyskytují ve vzduchu.

V části své práce věnující se metabolicky efektivnímu přenosu informace jsem se zaměřil především na roli inhibičních neuronů v efektivním přenosu informace. Pomocí matematické analýzy a simulací Monte Carlo modelů spikujících neuronů jsem ukázal, jak může vstup z presynaptických inhibičních neuronů snížit variabilitu post-synaptického neuronu přes jednotlivé pokusy, a zobecněním těchto výsledků na rekurentní neuronovou síť jsem ilustroval, jak může variabilita přes pokusy klesat s nástupem podnětu, což je jev známý jako zhášení neuronové variability. Informačně-teoretická analýza však ukázala, že vstup z inhibičních neuronů v podobě inhibiční zpětné vazby s nástupem podnětu přinese významné zlepšení metabolicky účinného přenosu informace pouze tehdy, pokud je informace přenášena populací rekurentně propojených neuronů, nikoliv jediným neuronem.

Abych pochopil obecné principy, kterými se řídí nervové kódování, zaměřil jsem se na nervovou aktivitu čichového systému hmyzu. Analyzoval jsem lokální polní potenciály (LFP) a aktivitu spikování hmyzích ORN stimulovaných novým zařízením pro doručování pachů, které je schopné časově přesně doručit podnět. Tyto nové záznamy ukázaly, že

ORN můry jsou mnohem schopnější kódovat délku trvání podnětu, než se dosud předpokládalo. Ukázalo se, že vlastnosti ORN můry jsou velmi podobné vlastnostem většiny ORN octomilky, což umožňuje sjednotit výzkum na těchto druzích. Na základě záznamů LFP jsem zkonstruoval minimální model ORN můry, který spolehlivě popisuje její aktivitu, přičemž využívá pouze několik interpretovatelných parametrů.

Jednoduchý a přenositelný model, který dokáže popsat aktivitu ORN, je nezbytný pro vytvoření integrativního modelu čichového systému hmyzu. Takový model by mohl být využit ke studiu informační metabolické účinnosti celého systému a k analýze, zda za určitých podmínek vysoká frekvence akčních potenciálů v anténním laloku skutečně napomáhá informačně-metabolické účinnosti. Výsledky mé práce jsou tedy krokem vpřed k pochopení obecných principů řídících nervový kód.

Résumé en français

Pour la plupart des neurones, l'information qu'ils transmettent est contenue dans le décours temporel d'émission de leurs impulsions électriques, appelées potentiels d'action. On ne sait pas encore bien décrypter ce "code neuronal". L'hypothèse du codage efficace propose que, sous l'effet de la pression évolutive, les systèmes sensoriels ont évolué pour transmettre et traiter l'information de la manière la plus efficace possible. Toutefois, la notion d'efficacité semble varier selon les systèmes sensoriels. Les neurones corticaux maintiennent une faible fréquence d'émission de potentiels d'action pour minimiser les dépenses métaboliques. Il en va de même pour les neurones récepteurs olfactifs des insectes (NRO, première couche du système olfactif). Les neurones du lobe antennaire des insectes (deuxième couche du système olfactif), en revanche, utilisent pleinement la gamme possible d'activité d'émission de potentiels d'action pour optimiser le codage olfactif. Dans ma thèse, j'ai étudié comment des neurones corticaux uniques et leurs populations peuvent transmettre et traiter des informations, tout en maintenant des dépenses métaboliques faibles, et aussi comment le système olfactif des insectes encode les informations sur les odeurs détectées dans l'air.

Dans la partie de ma thèse consacrée à la transmission métabolique efficace de l'information, j'ai principalement analysé la contribution des neurones inhibiteurs. En généralisant ces résultats à un réseau de neurones récurrents, j'ai illustré comment la variabilité d'un essai à l'autre peut diminuer avec l'apparition d'un stimulus, un phénomène connu sous le nom de "neural variability quenching" (atténuation de la variabilité neuronale). Toutefois, une analyse théorique de l'information a montré que l'apport des neurones inhibiteurs sous la forme d'une rétroaction inhibitrice lors de l'apparition d'un stimulus n'améliore significativement la transmission métabolique efficace de l'information que si cette information est transmise par une population de neurones connectés de manière récurrente, plutôt que par un seul neurone.

Pour comprendre les principes généraux régissant le codage neuronal, je me suis ensuite focalisé sur l'activité neuronale du système olfactif des insectes. J'ai analysé les potentiels de champ locaux (LFP) et l'activité d'émission de potentiels d'action de NRO d'insectes stimulés avec un

nouveau dispositif capable de délivrer des stimuli temporellement précis. L'utilisation de ce stimulateur a permis de démontrer que les NRO des papillons de nuit encodent mieux la durée du stimulus que ce qui était admis jusqu'à présent. Les propriétés des NRO de papillon de nuit se sont révélées très similaires à celles de la majorité des NRO de drosophile, ce qui permet d'unifier les recherches sur ces espèces. En utilisant les enregistrements des LFP, j'ai construit un modèle minimal du NRO du papillon de nuit qui décrit de manière fiable l'activité d'émission de potentiels d'action tout en utilisant seulement quelques paramètres interprétables.

Un modèle simple et transférable, capable de décrire la réponse des NRO, est essentiel pour construire un modèle intégratif du système olfactif des insectes. Un tel modèle pourra être utilisé pour étudier l'efficacité métabolique du codage de l'information par l'ensemble du système olfactif et analyser si, dans certaines conditions, les taux d'excitation élevés des neurones du lobe antennaire favorisent réellement cette efficacité. Les résultats de ma thèse constituent donc un pas en avant vers la compréhension des principes généraux régissant le code neuronal.

Introduction

Neurons are negatively charged compared to their surroundings. This imbalance in electrical charge allows neurons to communicate with electrical signals. Neurons communicate with each other by sending action potentials (spikes) along their axons. The action potential can then evoke a change in the electrical charge of a neuron (post-synaptic neuron), to which the neuron sending the action potential (pre-synaptic neuron) is connected with a synapse. Thus the external signal translates into a graded change of the neuron's membrane potential. For most neurons, an action potential is the only way for a neuron to communicate information further [1].

The message that a pre-synaptic neurons is sending to its post-synaptic neurons is then encoded in the timing of its action potentials. In my thesis I focus on analyzing how the information about an external stimulus, such as odor intensity in the air, is encoded in the sequence of action potentials (spike train) by individual neurons and their populations.

The rate coding hypothesis states assumes that a neuron encodes intensity of the stimulus in the number of action potentials it produces [2, 3, 4, 5]. Neurons implementing this strategy are said to use "rate code". In contrast to rate code, a cell is considered to use "temporal code" if the precise timing of action potentials contains essential information about the stimulus [1].

The efficient coding hypothesis asserts that neurons, under strong evolutionary pressure, are adapted to process the information from their natural surroundings efficiently [6]. Understanding how the information about the stimulus is encoded is essential for understanding the evolutionary pressures on the neural system. A popular approach to evaluating the efficiency of information processing is using Shannon's information theory [7]. Using Shannon's information theory we can use entropy-based measures to rigorously calculate the amount of information that can be contained in the neuronal response or the maximal amount of information that can be encoded in the response about the stimulus. Recordings from the retina of the blow fly showed that the stimulus-response relationship of the neurons is such that the entropy of the

response is maximized by a stimulus distribution that is very close to the contrast distribution observed in its natural environment, supporting the hypothesis that neurons evolved to encode the maximum amount of information possible. A similar entropy maximization principle has been observed in the *Drosophila* antennal lobe, the secondary layer of olfactory signal processing in insects [8, 9, 10].

When presented with an identical stimulus repeatedly, a neuronal response may be different during each trial. Such noise decreases the amount of information that a single neuron or a population of neurons can reliably transmit. It is, therefore, essential to understand the trial-to-trial variability of the neural system. A number of studies, therefore, analyzed both theoretically and experimentally the trial-to-trial variability in various neurons and neuronal models, showing that the trial-to-trial variability can be in a large portion of neurons described by a Poisson-like activity with a Fano factor close to one [11, 12, 13, 14, 15]. Interestingly, experimental studies also showed that the trial-to-trial variability may decrease with the stimulus onset [16, 17], a phenomenon which we studied theoretically [18].

In contrast to the observations in the blow fly retina and *Drosophila* antennal lobe, cortical neurons do not seem to maximize the amount of encoded or transmitted information. Instead, they seem to balance maximization of information transmission and minimization of energy consumption [19, 20, 21, 22, 23].

Based on the observation in cortical neurons, suggesting that the cortex maximizes transmitted information with constraints on the metabolic expenses, a number of studies investigated the maximization of information-per-cost in single neurons [24, 25, 26, 27, 28, 29]. showed that the balance between excitatory and inhibitory synaptic currents observed in *in-vivo* recordings of the cortex [30, 31] maximizes the information-per-cost in neurons using temporal code. This study, however, only considered a constant intensity input and did not analyze the effects of the external stimulus and the effect of its randomness on the trial-to-trial variability of the neuron and how the external stimulus is encoded.

In [32], we modeled information transmission by single neurons, with spontaneous activity generated by the background input with balanced excitatory and inhibitory synaptic currents as in [25], but receiving an

additional stimulus signal on top of this background input and studied the effect of different model parameters on the mutual information between the stimulus and the response with metabolic constraints. Among other parameters, we studied how the stimulus-associated inhibition affects metabolically efficient information transmission by the neurons and found that compared to other parameters, such as spontaneous activity, the stimulus-associated inhibition has only a minor effect.

Further, in [33] we studied the effect of stimulus-associated inhibition on metabolically efficient information transmission by populations of recurrently connected neurons. In neural populations the efficiency of information transmission is hindered by noise correlations among the neurons [34]. Inhibitory feedback reduces these correlations [35, 36, 37]. However, the inhibitory feedback is costly. Therefore, we investigated whether using the inhibitory feedback to reduce the noise correlations is metabolically efficient for populations of neurons encoding information in their averaged activity.

We also studied information transmission by the insect olfactory system. The insect olfactory system is a good system for studying efficient coding, since the neural structures are relatively simple, compared to cortical circuits, and in particular, male moth olfactory receptor neurons (ORNs) sensitive to their sex pheromone have a very specialized purpose, which is navigation to a conspecific female.

To conduct similar computational studies with moth olfactory receptor neurons as we did with cortical neurons we would need a spiking ORN model reproducing their responses to olfactory stimuli. However, studying the response dynamics of moth olfactory receptor neurons to pheromone stimulation is complicated due to difficulties with the precise delivery of odor molecules with low volatility, such as pheromones [38].

We built a new odor delivery device that solved the previously encountered issues and studied the responses of male moth olfactory receptor neurons (ORNs) to pheromone stimulation [39]. The observed responses differed from responses previously described in the literature [40, 41, 42, 43] and are similar to responses observed in *Drosophila* ORNs [44, 45, 46, 47]. We used these recordings to build a reliable model reproducing the firing rate responses to various stimuli [39]. Extending this model to include a spiking activity is a currently ongoing effort. A

brief report documenting these efforts is also a part of this manuscript.

The thesis is based on four published works and two unpublished reports. In the following sections, each of those works is briefly described, including the used methods.

1 The stabilizing effect of inhibition

Attachment I

Upon stimulus presentation, cortical neurons receive both excitatory and inhibitory input [16]. Each neuron typically receives input from many pre-synaptic neurons, and the timing of the pre-synaptic action potentials will differ in each trial with the same stimulus. Such noise in the input to the neuron leads to noise in the output of the neuron [48]. Comparing a situation where a neuron is excited only by the excitatory input with a situation where the neuron is excited to the same level by combined excitatory and inhibitory input, in the latter case, more pre-synaptic action potentials are necessary to excite the neuron, which implies higher input noise. Intuitively, the higher input noise should lead to higher trial-to-trial variability of the output. Monier et al. [16] observed that the fluctuation of the membrane potential in the neurons in the cat visual cortex decreased after stimulus onset, even when the mean membrane potential of the neuron remained unchanged. This is counter-intuitive due to the higher input noise associated with the inhibitory input.

We analyzed the standard equation describing the subthreshold membrane potential:

$$C\frac{\mathrm{d}V}{\mathrm{d}t} = -g_L(V - E_L) + I_{\mathrm{syn}}(t), \tag{1}$$

where V is the membrane potential, E_L is the resting potential, g_L is the leaky conductance, and $I_{\mathrm{syn}}(t)$ is the synaptic current. We modeled the synaptic current, evoked by excitatory and inhibitory pre-synaptic action potentials occurring at times $\mathcal{T}_{\mathrm{exc}} = \{t^1_{\mathrm{exc}}, t^2_{\mathrm{exc}}, \dots\}$ and $\mathcal{T}_{\mathrm{inh}} = \{t^1_{\mathrm{inh}}, t^2_{\mathrm{inh}}, \dots\}$ respectively, with different levels of biological realism:

- Without reversal potentials; without synaptic filtering

$$I_{\mathrm{syn}}(t) = \sum_{t_s \in \mathcal{T}_{\mathrm{exc}}} \frac{\Delta V_{\mathrm{exc}}}{C} \delta(t - t_s) + \sum_{t_s \in \mathcal{T}_{\mathrm{inh}}} \frac{\Delta V_{\mathrm{inh}}}{C} \delta(t - t_s), \quad (2)$$

where $\Delta V_{\mathrm{inh}} \leq 0 \leq \Delta V_{\mathrm{exc}}$ are discontinuous jumps of the membrane potential V.

- With reversal potentials; without synaptic filtering

$$\begin{aligned} I_{\mathrm{syn}}(t) = &\sum_{t_s \in \mathcal{T}_{\mathrm{exc}}} a_{\mathrm{exc}}(E_{\mathrm{exc}} - V)\delta(t - t_s) + \\ &+ \sum_{t_s \in \mathcal{T}_{\mathrm{inh}}} a_{\mathrm{inh}}(E_{\mathrm{inh}} - V)\delta(t - t_s), \end{aligned} \quad (3)$$

where E_{exc}, E_{inh} are synaptic reversal potentials, a_{exc}, a_{inh} are scaling constants.

- Without reversal potentials; with synaptic filtering

$$I_{\mathrm{syn}}(t) = I_{\mathrm{exc}}(t) + I_{\mathrm{inh}}(t), \quad (4)$$

$$\frac{\mathrm{d}I_{\mathrm{exc}}}{\mathrm{d}t} = -\frac{I_{\mathrm{exc}}}{\tau_{\mathrm{exc}}} + \sum_{t_s \in \mathcal{T}_{\mathrm{exc}}} b_{\mathrm{exc}} \delta(t - t_s), \quad (5)$$

$$\frac{\mathrm{d}I_{\mathrm{inh}}}{\mathrm{d}t} = -\frac{I_{\mathrm{inh}}}{\tau_{\mathrm{inh}}} + \sum_{t_s \in \mathcal{T}_{\mathrm{inh}}} b_{\mathrm{inh}} \delta(t - t_s), \quad (6)$$

where τ_{exc}, τ_{inh} are filtering time constants, b_{exc}, b_{inh} are discontinuous jumps in the synaptic currents.

- With reversal potentials; with synaptic filtering

$$I_{\mathrm{syn}}(t) = -g_{\mathrm{exc}}(t)(V - E_{\mathrm{exc}}) - g_{\mathrm{inh}}(t)(V - E_{\mathrm{inh}}) \quad (7)$$

$$\frac{\mathrm{d}g_{\mathrm{exc}}}{\mathrm{d}t} = -\frac{g_{\mathrm{exc}}}{\tau_{\mathrm{exc}}} + \sum_{t_s \in \mathcal{T}_{\mathrm{exc}}} c_{\mathrm{exc}} \delta(t - t_s), \quad (8)$$

$$\frac{\mathrm{d}g_{\mathrm{inh}}}{\mathrm{d}t} = -\frac{g_{\mathrm{inh}}}{\tau_{\mathrm{inh}}} + \sum_{t_s \in \mathcal{T}_{\mathrm{inh}}} c_{\mathrm{inh}} \delta(t - t_s), \quad (9)$$

where c_{exc}, c_{inh} are discontinuous jumps in the synaptic conductances g_{exc} and g_{inh}.

We showed that only if the synaptic current is modeled with reversal potentials and synaptic filtering, decreased membrane potential fluctuations with stimulus onset may be observed.

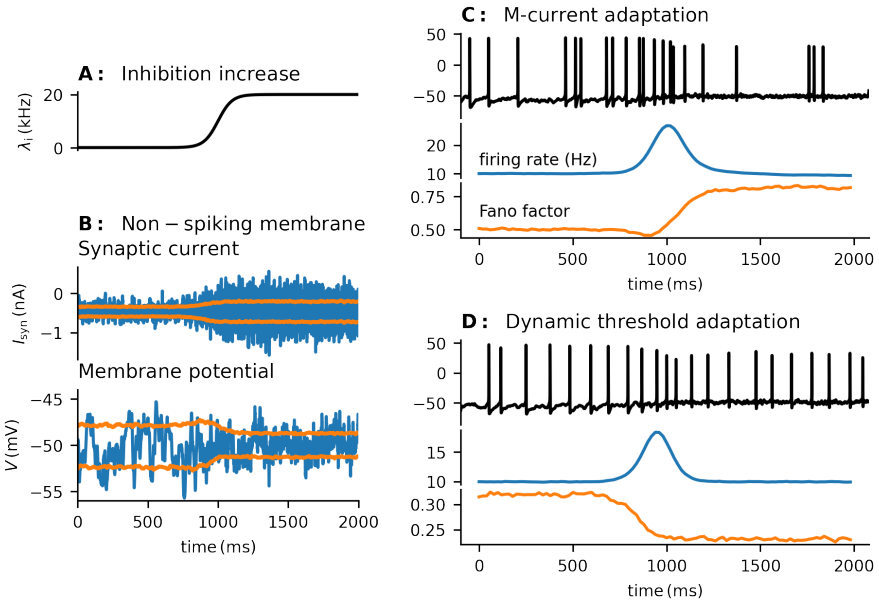

Figure 1: The stabilizing effect of inhibition. During a 2 s long simulation the intensity of inhibitory input increases from 0 kHz to 20 kHz. The pre-synaptic spike trains are modeled as Poisson point processes. The intensity of the excitatory input is increased simultaneously with the inhibition to keep the mean membrane potential (**B**) or the steady-state firing rate (**C-D**) constant. With the stronger input, fluctuations of the synaptic current increased (standard deviation highlighted in orange), but fluctuations of the membrane potential decreased. In the case of the firing activity, trial-to-trial variability decreased with the stronger stimulus only if spike frequency adaptation was modeled as a dynamic threshold (**C-D**).

The stimulus onset has been shown to decrease not only the trial-to-trial variability of the membrane potential but also the trial-to-trial variability of the firing activity [17] as measured by the Fano factor,

a phenomenon known as neural variability quenching. We analyzed whether this might be caused by the decreased membrane potential fluctuations associated with the stimulus onset. We found that the effect of the increased inhibitory input depends on the spike frequency adaptation (SFA) mechanism of the neuron.

We introduced a firing threshold to the Eq. (1). To model SFA, we either introduced a hyperpolarizing current in the Eq. (1), activating with depolarization and/or firing activity, or we made the firing threshold dependent on firing activity. We showed that only in the latter case the stimulus onset can decrease trial-to-trial variability of the firing activity. We also achieved similar effects with Hodgkin-Huxley type neuronal models (Fig. 1C-D).

2 Neural variability quenching in networks

Attachment II

The above discussed results were published in *Physical Review E* [18]. In the published work, we studied the properties of single neurons and simulated the stimulus onset as a simultaneous increase in the excitatory and inhibitory input at different ratios. To understand better the neurons' behavior with stimulus onset, it is beneficial to study the single neuron behavior in the context of a recurrent neural network in the sensory cortex with different neurons having different stimulus preferences and thus reproduce the experimental conditions as in [16] and [17]. The stimulus would be represented by an increased input intensity from thalamocortical synapses, with the increase dependent on the preferred stimulus and the associated increase in inhibitory input given by the network properties.

We started extending the published results in this direction. We considered a recurrent neural network of 10000 neurons, with 7500 neurons excitatory and 2500 inhibitory. Each neuron was modeled as an exponential leaky integrated-and-fire neuron [49, 50, 51] (i.e., an extra exponential term was added to the Eq. (1)), and the probability of a connection from one neuron to another was set to 5% [52]. Analogously to [18], we compared two types of networks, specified by two types of SFA of the neurons: dynamic threshold SFA and after-hyperpolarization

currents (AHP) SFA.

With the stimulus onset, each neuron received an input of different intensity, mimicking different preferred stimulus for each neuron. After the stimulus onset, some neurons increased their firing activity, some neurons decreased their firing activity and for some neurons, their firing activity remained approximately the same as before the stimulus onset. By comparing the trial-to-trial variability of neurons with approximately unchanged firing activity, we showed that only if the SFA is implemented by modeling a dynamic firing threshold, the trial-to-trial variability decreases with the stimulus onset.

Our results illustrate the importance of considering synaptic filtering and reversal potentials in neural modeling and extend our understanding of the effects of using different SFA mechanisms on the input-output properties of neural models [53]. Moreover, we theoretically explained the experimentally observed decrease of membrane potential fluctuations and provide a possible mechanism of decreased Fano factor with the stimulus onset.

3 Efficient coding by individual cortical neurons

Attachment III

Given that all the information a neuron passes on is contained within its output spike train, a model reproducing the neuron's response to a stimulus can be a proxy for conducting experiments. This is especially useful for evaluating the information transmission capabilities of neurons because such studies require large amounts of data, which are costly and lengthy to obtain experimentally. Numerous studies used mathematical neuronal models to evaluate the theoretical limits on information transmission. However, these studies typically dealt with simplified models with simplified inputs, which do not represent well the true behavior of neurons [54, 22, 23, 24, 27, 28, 29] or with biophysical models, which are difficult to generalize [26].

A gap between those model types was somewhat filled by the Multi-timescale Adaptive Threshold (MAT) model [55], modeling the SFA at two separate time scales. To obtain the MAT model, Eq. (1) is equipped

with a firing threshold $V_T(t)$ described by

$$V_T(t) = \sum_k H(t - t_k) + \omega, \tag{10}$$

$$H(t) = \sum_{j=1}^{2} \alpha_j \exp(-t/\tau_j), \tag{11}$$

where t_k are the previous spikes of the neuron, α_j is the discontinuous jump of the j-th threshold component upon spike firing, which then decays to zero exponentially with a time constant τ_j. The MAT model can precisely predict the timings of individual spikes of cortical neurons [55, 56, 57, 58] with only a modest number of free parameters. We used this model to evaluate the limits of metabolically efficient information transmission by neurons and to investigate the effect of changing the free parameters, which can be directly related to the neurons' properties.

We used mutual information to estimate the information transmission capabilities of a neuron [7, 54, 59, 60]:

$$I(X;Y) = H(Y) - H(Y|X), \tag{12}$$

where X is a random variable representing the stimulus (described by a probability distribution $p(x)$), Y is a random variable representing the response (number of action potentials in the coding time window Δ), $H(Y)$ is the entropy of the response random variable and $H(Y|X)$ is the noise entropy.

Due to costs associated with firing action potentials and reversing excitatory synaptic currents, the input probability distribution $p(x)$ is associated with an average cost of the neural activity W_p [61, 62]. We can then define a capacity-cost function $C(W)$ and information-metabolic efficiency E:

$$C(W) = \max_{\substack{p(x) \\ W_p < W}} I(X;Y), \tag{13}$$

$$E = \frac{C(W^*)}{W^*}, \tag{14}$$

$$W^* = \arg\max_W \frac{C(W)}{W}, \tag{15}$$

where the maximization in the Eq. (13) runs over all possible input distributions satisfying the condition $W_p < W$.

In accordance with some of the previous studies, we assumed that the "optimal regime" is such that it allows the transmission of as much information as possible per unit of energy (molecule of ATP), i.e., the input distribution is such that the information-metabolic efficiency (Eq. 14) is reached.

We studied the effect of the following neuronal and coding properties on the information-metabolic efficiency:

- Spike firing patterns,
- Stimulus-associated inhibitory input,
- Coding time window Δ,
- Spontaneous activity of the neuron.

We found that while the information-metabolic efficiency (Eq. 14) was robust towards the changes in the inhibition excitation balance and to the change in model parameters responsible for the spike firing patterns, the coding time window and spontaneous activity of the neuron had significant effects on the information-metabolic efficiency. Neurons with the lowest spontaneous activity had the highest values of information-metabolic efficiency, and shorter coding time windows led to higher information-metabolic efficiency.

We showed that it holds from the information-theoretic principles that shorter time windows cannot decrease the mutual information if the neuron is considered to be a memoryless information channel. However, with a shorter coding time window, the response of the neuron is more affected by the previous stimulus than in the case of a longer coding time window, decreasing its signal-to-noise ratio, as the stimulus history introduced another source of stochasticity (Figure 8B in [32]). We found that despite the additional source of variability in the stimulus history, shorter coding time windows led to higher information-metabolic efficiency (Figure 8E in [32]).

We used 34 sets of parameters obtained by fitting 34 neurons from layers 2/3 and 5 of the rat motor cortex [55, 63] (provided by professor

Ryota Kobayashi) to investigate the role of different parameters on the efficiency of information transmission. For a fixed coding time window, the information-metabolic efficiency was given mainly by the neurons' spontaneous firing rate due to the background network activity [64, 31], which is in turn given by the neurons' long-term adaptation properties (namely the magnitude of α_2 in the Eq. (11)) and their resting threshold for action potential initiation (ω in Eq. (10)). More detailed properties (e.g., the tendency to burst - fire rapidly many action potentials during a short period) turned out to be of lesser importance.

The results of our study were published in the journal PLoS Computational Biology [32].

4 Efficient coding by populations cortical neurons

Attachment IV

In the above-discussed study, among other parameters, we analyzed the effect of the stimulus-associated inhibitory input on metabolically efficient information transmission. While we observed that in some cases higher inhibition-to-excitation ratio may decrease the trial-to-trial variability of the response (see also [18]), this decrease was not sufficient to balance out the increased costs of synaptic currents and decreased coding range of the neurons. Yet, an increase in excitatory input intensity due to an external stimulus is typically accompanied by a simultaneous increase in the inhibitory input due to the excitation of inhibitory neurons [16], and it is unclear if and how the inhibition aids metabolically efficient information transmission.

However, inhibition is likely to play a much more important role on the level of whole neural populations instead of individual neurons. Inhibitory feedback can decrease the noise correlations and subsequently the trial-to-trial variability of the total population activity [65, 34, 35, 36, 37].

To analyze the impact of the inhibitory feedback on the rate coding capabilities of neural populations, we modeled a recurrent spiking neural network with 800 excitatory and 200 inhibitory neurons, representing a small cortical area (Fig. 2A). Similarly, as in the above-discussed

study, the neurons were receiving a balanced excitatory and inhibitory input, representing the input from neighboring cortical areas and an external input representing the excitatory input from the thalamocortical synapses. We modeled the thalamic input by considering an external population of 1000 excitatory neurons, making random connections onto the 800 excitatory and 200 inhibitory neurons. In our simulation, the inhibitory neurons provided the inhibitory feedback, and we varied the strength of the feedback by varying the strength of the recurrent connections.

We treated the whole population of 800 excitatory and 200 inhibitory neurons as a single information channel. We defined the output of this channel as the total number of post-synaptic action potentials observed in a time window $\Delta = 1\,\mathrm{s}$. Adding together the activity of many neurons can lead to a significant decrease in the trial-to-trial variability. However, noise correlations are induced by neurons sharing input from the same neurons in the external population. In the presence of noise correlations, the decrease in the signal-to-noise ratio will be lower [65]. We varied the noise correlations between neurons by varying the connection probability P_{ext} from the external neurons to the excitatory and inhibitory populations. High values of P_{ext} meant high noise correlations.

We considered the costs of the whole system. Therefore, on top of the costs of the excitatory and inhibitory subpopulations (the cost of synaptic currents and action potentials), we also considered the cost of the action potentials from the external population. With higher P_{ext}, more neurons are involved in exciting any neuron from the excitatory or inhibitory subpopulation. Therefore, the total activity of the external population can be lower to reach the same post-synaptic firing rate.

On the other hand, increasing the inhibitory feedback by increasing the strength of the recurrent connections decreases the post-synaptic firing rate of the network, and stronger synaptic currents and stronger external input are needed to reach the same post-synaptic firing rate, compared to a network with weaker inhibitory feedback. Therefore, the cost of the neural activity of a network with stronger recurrent connections is higher.

In our work, we studied the balance between mutual information in metabolic costs. We found that high values of P_{ext} typically increase the

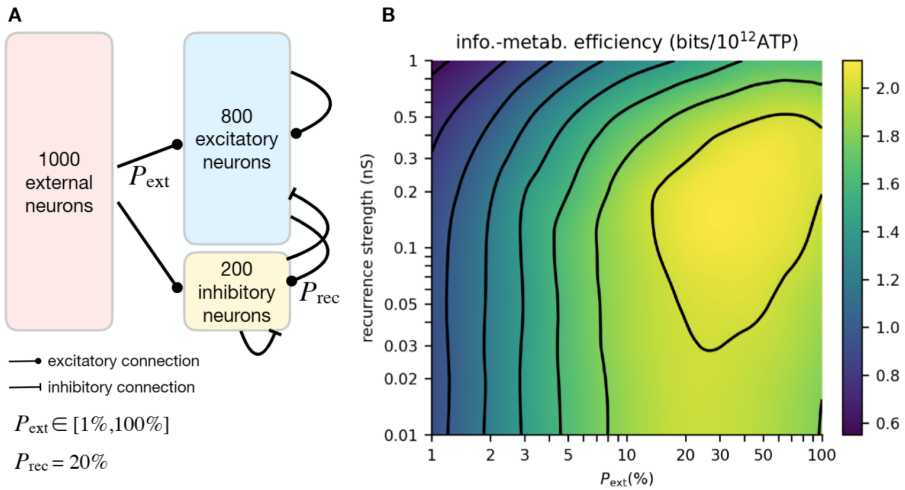

Figure 2: Metabolically efficient information transmission by a recurrent neural network. A: Schematic illustration of a network used to study the role of inhibition in metabolically efficient encoding by neural populations. Neurons from an external population make random excitatory connections on neurons in the excitatory and inhibitory populations. The connection probability P_{ext} was varied for different simulations between 1% and 100%, leading to different pair-wise correlations between the post-synaptic neurons. The probability of recurrent connections (ext to exc, ext to inh, inh to inh, inh to exc) was set to 20%, but the strength of those connections was varied. **B:** Contour plot of the information-metabolic efficiency for different values of P_{ext} and recurrence strength. The information-metabolic efficiency is the highest for P_{ext} between 20% and 50% and recurrence strength of approximately 0.2 nS, or 20% of the synapse strength from the external population.

information-metabolic efficiency of the system. With high values of P_{ext}, the information-metabolic efficiency can be further improved by strengthening the inhibitory feedback (Fig. 2B). Moreover, we showed that the neural system can decrease its energy consumption by decreasing the strength of the synaptic weights, a phenomenon observed experimentally

in food-restricted mice [66].

Results of our study are currently published in *bioRxiv* [33].

5 Temporal features encoding by moth olfactory receptor neurons

Attachment V

Studying insect olfaction is, in certain aspects, the ideal system to study how evolution shapes neural systems to adapt to their environment. The olfactory system is relatively simple, and specifically, moth olfactory receptor neurons need to be highly adapted to encode the temporal features of the pheromone plume. However, a lot is still unknown about what temporal features the system actually encodes, and studying the dynamics of the ORN response has been difficult in moths due to difficulties with delivering odor stimulus with a sharp onset, such as the moth might encounter in nature.

We developed a new odor-delivery device that can deliver sharp stimulus pulses even with odors with low volatility. We tested the precision of the odor delivery device with molecules detectable by a photo-ionization detector (PID).

Previous studies showed that the moth ORNs clearly detect the onset of the stimulus by responding to the sudden increase in odor concentration, but also observed a sustained response even after the stimulus offset [40, 41, 42, 43]. Such observations were surprising since it complicates the detection of the odor offset, a feature which was then thought to be performed in the antennal lobe [67, 41, 43, 68, 69]. With the new odor delivery device we observed that the moth ORNs can, in fact, detect the odor offset by a transient inhibitory phase, provided that the stimulus is sufficiently long (Fig. 3). Moreover, we showed that the response shape is independent of the stimulus concentration, which has important implications for odor identity discrimination [47] (Figure 5 in [39]).

For brief stimuli, the response of the ORNs continued after the stimulus offset. For pulses of duration below 200 ms the firing response continued for approximately 100 ms after the stimulus offset (Fig. 3). Previous studies showed that even though the response of ORNs is

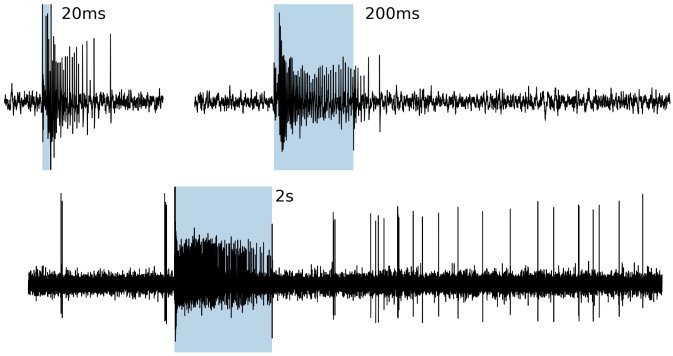

Figure 3: Spiking responses to constant stimuli of different durations. After the short stimulus (20 ms) the ORN continues to fire for approximately 100 ms after the stimulus offset. After the 2 s stimulation, the stimulus offset is immediately followed by a transient inhibition.

sustained after the stimulus offset, the PNs do exhibit the transient inhibition marking the stimulus offset, albeit with a delay of more than 100 ms [67]. We were therefore interested if the encoding of the stimulus offset is further sharpened at the AL level. We used the ORN firing rates as an input to a moth antennal lobe model [68, 69] and did not observe any improvement in stimulus offset detection. Although recordings from the antennal lobe neurons will be necessary to show that the stimulus offset detection is not improved, we hypothesize that the stimulus offset detection is not necessary for very brief encounters with the odor. This correlates with the observed behavior of flying insects. Moths were shown to continue flying in a straight line towards the source when presented with a pulsating stimulus [70, 71, 72]. Particularly, Mafra-Neto and Cardé [72] studied the behavior of the almond moth *Cadra cautella* and observed that the best navigation performance was achieved with a pulse duration 130 ms and a gap between pulses 83 ms. Instead, the prolonged response to very brief odor encounters might help the insect to register those encounters.

It has been known that the phasi-tonic response shape of ORNs originates from the adaptation processes in the spike-generating mecha-

nism [73]. However, the molecular origins of this adaptation are still unknown [74]. We proposed a new approach to fitting linear-nonlinear models to neural activity, which provides us insights into the timescales of input integration by the ORN and adaptation to the stimulus. Linear-nonlinear models are used to predict neuronal firing rates ν [1] and are described by a linear kernel K and a static non-linearity f. The firing rate predicted by the model is

$$\hat{\nu} = f((K * s)(t)), \tag{16}$$

where $s(t)$ is the time course of the stimulus. We searched for a kernel in the form of

$$K(t) = \sum_{\tau \in \boldsymbol{\tau}} \sum_{\alpha \in \boldsymbol{\alpha}} c_{\tau,\alpha} \frac{1}{\Gamma(\alpha)\tau^{\alpha}} t^{\alpha-1} e^{-\frac{t}{\tau}}, \tag{17}$$

where $\boldsymbol{\tau}$ and $\boldsymbol{\alpha}$ are sets of different time constants and shape parameters. We estimated the coefficients $c_{\tau,\alpha}$ with lasso regression. We used a rectifying linear function as the static nonlinearity f:

$$f(x) = \begin{cases} 0 & \text{for } x \leq 0, \\ x & \text{for } x > 0. \end{cases} \tag{18}$$

This approach overcomes issues imposed by elastic net regularization, commonly employed for fitting linear-nonlinear models [47, 75] by enforcing a continuous linear filter without oscillations while allowing high-frequency components in the linear filter. From the fitted parameters we inferred that the ORN firing response is shaped by adaptation processes in the soma at time scales of approximately 31 ms and 635 ms.

A low ratio of Na^+ to K^+ channels may make a neuron respond more phasically [76], and it was hypothesized that the phasicity on *Drosophila* ORNs is due to this mechanism [46]. The adaptation time scales inferred from our model are longer than the common adaptation time scales of Na^+ channels in insect ORNs (approximately 5 ms [77]). Slower adaptation of the Na^+ channels would be necessary to result in the observed responses. Further experiments focused on identifying possible adaptation of insect ORN Na^+channels at longer timescales should be performed to understand better whether the hypothesis proposed by Nagel and Wilson [46] is correct.

The two separate adaptation time scales also explain the prolonged response to brief stimuli. During the short stimulus, the slow adaptation does not activate sufficiently to rapidly terminate the response and therefore the ORN continues to fire action potentials after the stimulus offset.

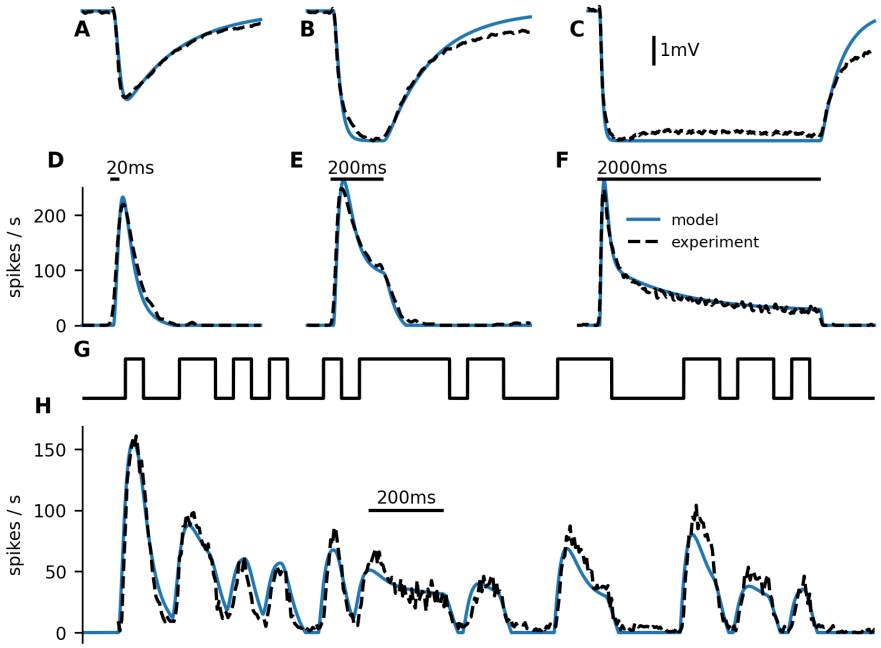

Figure 4: Odor-to-firing rate model. A-C: Prediction of LFP responses to stimuli of different durations. The blue line shows the transduction model prediction, dashed black line is the average LFP observed from SSR. **D-F:** Combining the transduction model with the linear-nonlinear model leads to an odor-to-firing rate model, which accurately predicts firing responses to the different stimulus durations. **G-H:** The odor-to-firing rate model also reliably predicts the firing rate in response to a fluctuating stimulus. **G** shows the stimulus being switched between ON and OFF with a constant odor concentration.

Studies using ORN firing rates as an input to models of higher brain centers typically model the ORN input as piece-wise exponential

functions with slow firing rate decay after the stimulus offset [78, 68, 69]. We combined our linear-nonlinear model with a simple transduction model [46] to obtain a reliable odor-to-firing rate model containing only a small number of parameters that can be used in computational studies of higher brain centers. The model also incorporates the newly discovered properties of moth ORNs.

Results of our study are currently published in *bioRxiv* [39].

6 Spike firing patterns of olfactory receptor neurons

Attachment VI

The literature so far has paid attention mainly to the time course of firing rates in olfactory receptor neurons and not so much to the spike firing patterns and the subsequent trial-to-trial variability of the response. A common assumption is that the spike firing activity can be described by an inhomogeneous Poisson process [78, 79, 80, 68, 69]. Such an approach may be justified in some cases since the pooled activity of all neurons could be approximated by an inhomogeneous Poisson process. However, synapses from ORNs to the projection neurons in the antennal lobe (PNs) are known to undergo short-term synaptic depression. Temporal correlations in the spike trains are known to affect signal processing by such depressing synapses [81], and temporal correlations in the ORN firing activity may, therefore, significantly affect how the signal is passed on from the ORNs to the PNs. Consequently, a good statistical description of the spike firing patterns is needed to understand the effect of these patterns on information transmission from the ORNs to the PNs.

We analyzed the trial-to-trial variability and spike firing patterns of moth ORNs. We found that most ORNs exhibit a bursting spike firing pattern, as seen in inter-spike interval (ISI) histograms on a logarithmic scale (Fig. 5A). We could describe the short ISIs within a burst by the inverse Gaussian distribution, while the inter-burst intervals (IBIs) could be described with a gamma distribution (Fig. 5B-C).

The moth ORNs show an elevated spontaneous activity following the transient inhibition after the stimulus offset (rebound activity). The

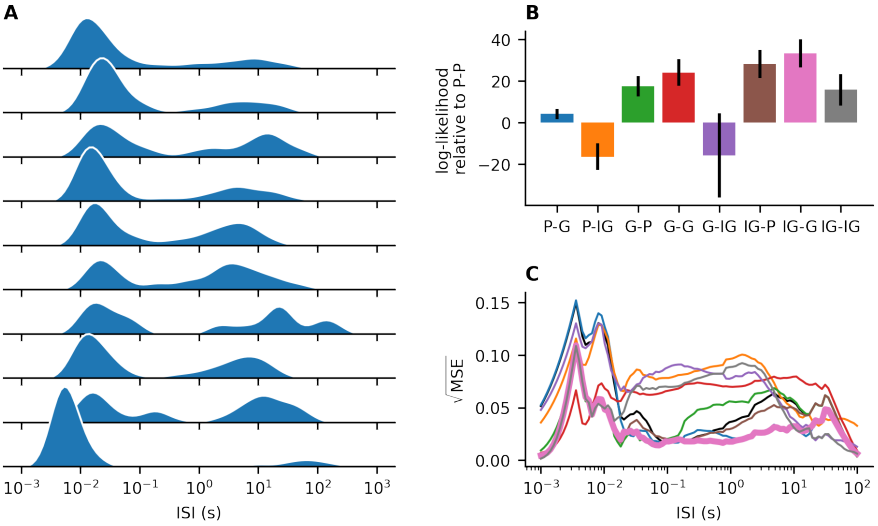

Figure 5: Statistical description of spontaneous activity of moth ORNs. A: Distributions of ISIs for 10 different ORNs. The distributions have two modes, one corresponding to ISIs within a burst and the second to ISI between two bursts. **B:** We fit mixtures of two distributions to the ISIs by the maximum likelihood method. The shown values are average log-likelihood values relative to the exponential-exponential distribution. P - exponential distribution, G - gamma distribution, IG - inverse Gaussian distribution. The vertical bar indicates the standard error. The best fit was a mix of inverse Gaussian distribution for the bursts and gamma distribution for the inter-burst intervals. **C:** Root of the square error between the cumulative distribution function of the fitted distribution and the empirical cumulative distribution function, averaged over the neurons. The colors correspond to **B**, the IG-G model is in bold, and the P-P model is in black.

elevated activity slowly returns to its original level on the time scale of minutes. This activity also clearly shows two modes of ISIs which can again be described by inverse Gaussian and gamma distributions. We applied the time rescaling theorem [82, 83, 84] to fit a double exponential

decay of the firing rate to the rebound activity. The mixture of inverse Gaussian and gamma distributions with time-dependent intensities provides a good fit for the rebound activity, as illustrated in the attached report.

We showed that the activity of moth ORNs can be described by a mixture of two stochastic point processes with inverse Gaussian and gamma distributions. We were able to fit well the spontaneous activity and the rebound activity. Whether a similar model can describe the response during stimulation remains to be analyzed. If we can describe the full behavior or an ORN with an inhomogeneous point process, we can use it to extend the linear-nonlinear models with a spiking activity, simulate realistic spike trains and thus obtain a spiking odor-to-firing rate model. Such a model could then be used as an input to AL models to understand the role of the observed spike firing patterns in signal transmission.

Conclusion

In my thesis, I studied the encoding of neural information by different systems and conditions and the information-metabolic efficiency of the encoding. I showed that while inhibitory feedback does not help increase the efficiency of encoding by single neurons, it may improve the information-metabolic efficiency of neural populations. I showed that the information-metabolic efficiency is crucially affected by the spontaneous activity of the neuron and its cost.

Such observation inspires questions about the importance of the spontaneous activity. In the higher brain areas, the spontaneous activity can be important, for example, for memory consolidation [85]. Such function is unlikely, for example, in the periphery of the insect olfactory system. Accordingly, the spontaneous activity of the pheromone-sensitive moth ORNs is very low [86, 41, 39]. However, this is not always the case across all ORN types and insect species. For example, moth ORNs sensitive to plant volatile compounds and *Drosophila* ORNs may exhibit much higher spontaneous firing rates [87]. The ORNs responding to plant volatile compounds typically respond to a broad range of odors, and the odor's identity is then encoded by the combinatorial code (one ORN

recognizes multiple odor molecules, and one odor molecule is recognized by multiple ORNs) [88]. Although most ORN-odor combinations result in excitation of the ORN, some ORN-odor combinations decrease the spontaneous activity, helping discriminate different odors [87, 89]. The metabolic importance of keeping the spontaneous activity low might be why the spontaneous activity is not even higher and odor-induced inhibition not more common. Pheromone-sensitive ORNs, on the other hand, do not need to encode the odor identity, and higher spontaneous activity might not be beneficial for stimulus encoding.

In the analysis of metabolically efficient neural coding, I focused predominantly on models of cortical neurons and neural networks. The proposed model of ORN is a step towards conducting similar studies in the moth olfactory system. Although models of moth ORNs and PNs reproducing the firing rates of the neurons and their heterogeneity have been proposed [75, 90], these models focused only on the firing rates and although the model by Levakova et al. [90] is a spiking model, it does not aim to reproduce the spiking patterns of the ORNs and their trial-to-trial variability, properties essential for understanding the efficiency of information encoding and effect on neurons downstream. The model by Jacob et al. [75] could be extended to take into account the trial-to-trial variability of the neurons in the same way as the linear-nonlinear model proposed in this thesis. However, the portability of this model is limited, as the knowledge of the full-time course of the filters (or the time course of their principal components) is necessary to replicate the results.

Firing profiles of the ORN responses and behavior of the insects suggest that greater emphasis is put on encoding the odor onset and odor offset when encoding the information about the stimulus. Further downstream, PNs are less sensitive to differences in odor concentration than ORNs [41, 91, 92]. Therefore we can assume that the goal of the olfactory system is not to transmit as much information as possible about the stimulus to the higher brain areas. Instead, the ORNs and the neurons in the AL clearly select which information should be passed on. An alternative approach is then to evaluate the encoding efficiency of the specific features of the stimulus, such as the durations of blanks between two subsequent odor encounters [93].

Ultimately, however, the goal of the insect in the navigation problem

is to locate the source. The efficiency of the olfactory system should therefore be evaluated as the efficiency in locating the source. Simulations of insect behavior based on olfactory system activity have been shown to be useful in comparing different navigation strategies [94, 95, 96] and in testing how properties of the olfactory system affect the navigation efficiency [96, 97]. Having a reliable model of the olfactory system is essential for such studies. Enforcing metabolic constraints on the navigation task could then help explain from the first principles why PNs seem to maximize the entropy of their output while ORN firing rates remain low.

Bibliography

[1] Dayan P, Abbott LF. Theoretical Neuroscience: Computational and Mathematical Modeling of Neural Systems. The MIT Press; 2005.

[2] Adrian ED. The impulses produced by sensory nerve endings. J Physiol. 1926;61(1):49–72. doi:10.1113/jphysiol.1926.sp002273.

[3] Adrian ED, Zotterman Y. The impulses produced by sensory nerve-endings. J Physiol. 1926;61(2):151–171. doi:10.1113/jphysiol.1926.sp002281.

[4] Adrian ED, Zotterman Y. The impulses produced by sensory nerve endings. J Physiol. 1926;61(4):465–483. doi:10.1113/jphysiol.1926.sp002308.

[5] Kandel ER, Jessell TM, Schwartz JH, Siegelbaum SA, Hudspeth AJ. Principles of Neural Science, Fifth Edition. Principles of Neural Science. McGraw-Hill Education; 2013.

[6] Barlow HB. Possible Principles Underlying the Transformations of Sensory Messages. In: Sensory Communication. The MIT Press; 1961. p. 217–234.

[7] Shannon C. A mathematical theory of communication. Bell system technical journal. 1948;27.

[8] Bhandawat V, Olsen SR, Gouwens NW, Schlief ML, Wilson RI. Sensory processing in the Drosophila antennal lobe increases reliability and separability of ensemble odor representations. Nat Neurosci. 2007;10(11):1474–1482. doi:10.1038/nn1976.

[9] Abbott LF, Luo SX. A step toward optimal coding in olfaction. Nat Neurosci. 2007;10(11):1342–1343. doi:10.1038/nn1107-1342.

[10] Kadakia N, Emonet T. Front-end Weber-Fechner gain control enhances the fidelity of combinatorial odor coding. eLife. 2019;8. doi:10.7554/eLife.45293.

[11] Tuckwell HC. Introduction to Theoretical Neurobiology. Cambridge University Press; 1988.

[12] Geisler WS, Albrecht DG. Visual cortex neurons in monkeys and cats: Detection, discrimination, and identification. Vis Neurosci. 1997;14(5):897–919. doi:10.1017/S0952523800011627.

[13] Gur M, Beylin A, Snodderly DM. Response Variability of Neurons in Primary Visual Cortex (V1) of Alert Monkeys. J Neurosci. 1997;17(8):2914–2920. doi:10.1523/JNEUROSCI.17-08-02914.1997.

[14] Shadlen MN, Newsome WT. The Variable Discharge of Cortical Neurons: Implications for Connectivity, Computation, and Information Coding. J Neurosci. 1998;18(10):3870–3896. doi:10.1523/jneurosci.18-10-03870.1998.

[15] Brunel N. Dynamics of Sparsely Connected Networks of Excitatory and Inhibitory Spiking Neurons. J Comput Neurosci. 2000;8:183–208. doi:https://doi.org/10.1023/A:1008925309027.

[16] Monier C, Chavane F, Baudot P, Graham LJ, Frégnac Y. Orientation and Direction Selectivity of Synaptic Inputs in Visual Cortical Neurons. Neuron. 2003;37(4):663–680. doi:10.1016/s0896-6273(03)00064-3.

[17] Churchland MM, Yu BM, Cunningham JP, Sugrue LP, Cohen MR, Corrado GS, et al. Stimulus onset quenches neural variability: a

widespread cortical phenomenon. Nat Neurosci. 2010;13(3):369–78. doi:10.1038/nn.2501.

[18] Barta T, Kostal L. Regular spiking in high-conductance states: The essential role of inhibition. Phys Rev E. 2021;103(2):022408. doi:10.1103/PhysRevE.103.022408.

[19] Levy WB, Baxter RA. Energy Efficient Neural Codes. Neural Comput. 1996;8(3):531–543. doi:10.1162/neco.1996.8.3.531.

[20] Treves A, Panzeri S, Rolls ET, Booth M, Wakeman EA. Firing rate distributions and efficiency of information transmission of inferior temporal cortex neurons to natural visual stimuli. Neural Comput. 1999;11(3):601–632.

[21] Balasubramanian V, Kimber D, Berry II MJ. Metabolically Efficient Information Processing. Neural Comput. 2001;13(4):799–815. doi:10.1162/089976601300014358.

[22] de Polavieja GG. Errors Drive the Evolution of Biological Signalling to Costly Codes. J Theor Biol. 2002;214(4):657–664. doi:10.1006/jtbi.2001.2498.

[23] de Polavieja GG. Reliable biological communication with realistic constraints. Phys Rev E. 2004;70(6). doi:10.1103/physreve.70.061910.

[24] Suksompong P, Berger T. Capacity Analysis for Integrate-and-Fire Neurons With Descending Action Potential Thresholds. IEEE Trans Inf Theory. 2010;56(2):838–851. doi:10.1109/tit.2009.2037042.

[25] Sengupta B, Laughlin SB, Niven JE. Balanced Excitatory and Inhibitory Synaptic Currents Promote Efficient Coding and Metabolic Efficiency. PLoS Comput Biol. 2013;9(10):e1003263. doi:10.1371/journal.pcbi.1003263.

[26] Kostal L, Kobayashi R. Optimal decoding and information transmission in Hodgkin-Huxley neurons under metabolic cost constraints. Biosystems. 2015;136:3–10. doi:10.1016/j.biosystems.2015.06.008.

[27] Xing J, Berger T, Sungkar M, Levy WB. Energy Efficient Neurons With Generalized Inverse Gaussian Conditional and Marginal Hitting Times. IEEE Trans Inf Theory. 2015;61(8):4390–4398. doi:10.1109/tit.2015.2444401.

[28] Sungkar M, Berger T, Levy WB. Mutual Information and Parameter Estimation in the Generalized Inverse Gaussian Diffusion Model of Cortical Neurons. IEEE Trans Mol Biol Multiscale Commun. 2016;2(2):166–182. doi:10.1109/tmbmc.2017.2656861.

[29] Sungkar M, Berger T, Levy WB. Capacity achieving input distribution to the generalized inverse Gaussian neuron model. In: 2017 55th Annual Allerton Conference on Communication, Control, and Computing (Allerton). IEEE; 2017.

[30] Paré D, Shink E, Gaudreau H, Destexhe A, Lang EJ. Impact of Spontaneous Synaptic Activity on the Resting Properties of Cat Neocortical Pyramidal Neurons In Vivo. J Neurophysiol. 1998;79(3):1450–1460. doi:10.1152/jn.1998.79.3.1450.

[31] Destexhe A, Rudolph M, Paré D. The high-conductance state of neocortical neurons in vivo. Nat Rev Neurosci. 2003;4(9):739–751. doi:10.1038/nrn1198.

[32] Barta T, Kostal L. The effect of inhibition on rate code efficiency indicators. PLoS Comput Biol. 2019;15(12):e1007545. doi:10.1371/journal.pcbi.1007545.

[33] Barta T, Kostal L. Shared input and recurrency in neural networks for metabolically efficient information transmission. bioRxiv. 2023; p. 2023.03.13.532471. doi:10.1101/2023.03.13.532471.

[34] Averbeck BB, Latham PE, Pouget A. Neural correlations, population coding and computation. Nat Rev Neurosci. 2006;7(5):358–366. doi:10.1038/nrn1888.

[35] Renart A, de la Rocha J, Bartho P, Hollender L, Parga N, Reyes A, et al. The Asynchronous State in Cortical Circuits. Science. 2010;327(5965):587–590. doi:10.1126/science.1179850.

[36] Tetzlaff T, Helias M, Einevoll GT, Diesmann M. Decorrelation of Neural-Network Activity by Inhibitory Feedback. PLoS Comp Biol. 2012;8(8):e1002596. doi:10.1371/journal.pcbi.1002596.

[37] Bernacchia A, Wang XJ. Decorrelation by Recurrent Inhibition in Heterogeneous Neural Circuits. Neural Comput. 2013;25(7):1732–1767. doi:10.1162/NECO_a_00451.

[38] Gorur-Shandilya S, Martelli C, Demir M, Emonet T. Controlling and measuring dynamic odorant stimuli in the laboratory. J Exp Biol. 2019;222(23):jeb207787. doi:10.1242/jeb.207787.

[39] Barta T, Monsempès C, Demondion E, Chatterjee A, Kostal L, Lucas P. Stimulus duration encoding occurs early in the moth olfactory pathway. bioRxiv. 2022; p. 2022.07.21.501055. doi:10.1101/2022.07.21.501055.

[40] Kaissling KE, Meng LZ, Bestmann HJ. Responses of bombykol receptor cells to (Z,E)-4,6-hexadecadiene and linalool. J Comp Physiol A. 1989;165(2):147–154. doi:10.1007/BF00619189.

[41] Jarriault D, Gadenne C, Lucas P, Rospars JP, Anton S. Transformation of the Sex Pheromone Signal in the Noctuid Moth Agrotis ipsilon: From Peripheral Input to Antennal Lobe Output. Chem Senses. 2010;35(8):705–715. doi:10.1093/chemse/bjq069.

[42] Grémiaux A, Nowotny T, Martinez D, Lucas P, Rospars JP. Modelling the signal delivered by a population of first-order neurons in a moth olfactory system. Brain Res. 2012;1434. doi:10.1016/j.brainres.2011.09.035.

[43] Rospars JP, Grémiaux A, Jarriault D, Chaffiol A, Monsempès C, Deisig N, et al. Heterogeneity and Convergence of Olfactory First-Order Neurons Account for the High Speed and Sensitivity of Second-Order Neurons. PLoS Comput Biol. 2014;10(12):e1003975. doi:10.1371/journal.pcbi.1003975.

[44] Kim AJ, Lazar AA, Slutskiy YB. System identification of Drosophila olfactory sensory neurons. J Comput Neurosci. 2011;30(1). doi:10.1007/s10827-010-0265-0.

[45] Kim AJ, Lazar AA, Slutskiy YB. Projection neurons in Drosophila antennal lobes signal the acceleration of odor concentrations. eLife. 2015;4. doi:10.7554/eLife.06651.

[46] Nagel KI, Wilson RI. Biophysical mechanisms underlying olfactory receptor neuron dynamics. Nat Neurosci. 2011;14(2):208–216. doi:10.1038/nn.2725.

[47] Martelli C, Carlson JR, Emonet T. Intensity Invariant Dynamics and Odor-Specific Latencies in Olfactory Receptor Neuron Response. J Neurosci. 2013;33(15). doi:10.1523/JNEUROSCI.0426-12.2013.

[48] Stein RB, Gossen ER, Jones KE. Neuronal variability: noise or part of the signal? Nat Rev Neurosci. 2005;6(5):389–397.

[49] Fourcaud-Trocmé N, Hansel D, van Vreeswijk C, Brunel N. How Spike Generation Mechanisms Determine the Neuronal Response to Fluctuating Inputs. J Neurosci. 2003;23(37):11628–11640. doi:10.1523/JNEUROSCI.23-37-11628.2003.

[50] Brette R, Gerstner W. Adaptive Exponential Integrate-and-Fire Model as an Effective Description of Neuronal Activity. J Neurophysiol. 2005;94(5):3637–3642. doi:10.1152/jn.00686.2005.

[51] Platkiewicz J, Brette R. A Threshold Equation for Action Potential Initiation. PLoS Comput Biol. 2010;6(7):e1000850. doi:10.1371/journal.pcbi.1000850.

[52] Zerlaut Y, Chemla S, Chavane F, Destexhe A. Modeling mesoscopic cortical dynamics using a mean-field model of conductance-based networks of adaptive exponential integrate-and-fire neurons. J Comput Neurosci. 2017;44(1):45–61. doi:10.1007/s10827-017-0668-2.

[53] Benda J, Maler L, Longtin A. Linear Versus Nonlinear Signal Transmission in Neuron Models With Adaptation Currents or Dynamic Thresholds. J Neurophysiol. 2010;104(5):2806–2820. doi:10.1152/jn.00240.2010.

[54] Stein RB. The Information Capacity of Nerve Cells Using a Frequency Code. Biophys J. 1967;7(6):797–826. doi:10.1016/s0006-3495(67)86623-2.

[55] Kobayashi R, Tsubo Y, Shinomoto S. Made-to-order spiking neuron model equipped with a multi-timescale adaptive threshold. Front Comput Neurosci. 2009;3:9. doi:10.3389/neuro.10.009.2009.

[56] Gerstner W, Naud R. How Good Are Neuron Models? Science. 2009;326(5951):379–380. doi:10.1126/science.1181936.

[57] Jahangiri AF, Gerling GJ. A multi-timescale adaptive threshold model for the {SAI} tactile afferent to predict response to mechanical vibration. In: 2011 5th International {IEEE}/{EMBS} Conference on Neural Engineering. IEEE; 2011.

[58] Kobayashi R, Kitano K. Impact of slow K+ currents on spike generation can be described by an adaptive threshold model. J Comput Neurosci. 2016;40(3):347–362. doi:10.1007/s10827-016-0601-0.

[59] Borst A, Theunissen FE. Information theory and neural coding. Nat Neurosci. 1999;2(11):947–957.

[60] McDonnell MD, Ikeda S, Manton JH. An introductory review of information theory in the context of computational neuroscience. Biol Cybern. 2011;105:55–70.

[61] Attwell D, Laughlin SB. An Energy Budget for Signaling in the Grey Matter of the Brain. J Cereb Blood Flow Metab. 2001;21(10):1133–1145. doi:10.1097/00004647-200110000-00001.

[62] Harris JJ, Jolivet R, Attwell D. Synaptic energy use and supply. Neuron. 2012;75(5):762–777.

[63] Isomura Y, Harukuni R, Takekawa T, Aizawa H, Fukai T. Microcircuitry coordination of cortical motor information in self-initiation of voluntary movements. Nat Neurosci. 2009;12(12):1586–1593. doi:10.1038/nn.2431.

[64] Destexhe A, Rudolph M, Fellous JM, Sejnowski TJ. Fluctuating synaptic conductances recreate in vivo-like activity in neocortical neurons. Neuroscience. 2001;107(1):13–24.

[65] Abbott LF, Dayan P. The Effect of Correlated Variability on the Accuracy of a Population Code. Neural Comput. 1999;11(1):91–101. doi:10.1162/089976699300016827.

[66] Padamsey Z, Katsanevaki D, Dupuy N, Rochefort NL. Neocortex saves energy by reducing coding precision during food scarcity. Neuron. 2022;110(2):280–296. doi:10.1016/j.neuron.2021.10.024.

[67] Jarriault D, Gadenne C, Rospars JP, Anton S. Quantitative analysis of sex-pheromone coding in the antennal lobe of the moth Agrotis ipsilon: a tool to study network plasticity. J Exp Biol. 2009;212(8):1191–1201. doi:10.1242/jeb.024166.

[68] Tuckman H, Patel M, Lei H. Effects of Mechanosensory Input on the Tracking of Pulsatile Odor Stimuli by Moth Antennal Lobe Neurons. Front Neurosci. 2021;15. doi:10.3389/fnins.2021.739730.

[69] Tuckman H, Kim J, Rangan A, Lei H, Patel M. Dynamics of sensory integration of olfactory and mechanical stimuli within the response patterns of moth antennal lobe neurons. J Theor Biol. 2021;509. doi:10.1016/j.jtbi.2020.110510.

[70] Willis MA, Baker TC. Effects of intermittent and continuous pheromone stimulation on the flight behaviour of the oriental fruit moth, Grapholita molesta. Physiol Entomol. 1984;9(3):341–358. doi:10.1111/j.1365-3032.1984.tb00715.x.

[71] Kennedy JS, Ludlow AR, Sanders CJ. Guidance system used in moth sex attraction. Nature. 1980;288(5790):475–477. doi:10.1038/288475a0.

[72] Mafra-Neto A, Cardé RT. Fine-scale structure of pheromone plumes modulates upwind orientation of flying moths. Nature. 1994;369(6476):142–144. doi:10.1038/369142a0.

[73] Kaissling KE, Strausfeld CZ, Rumbo ER. Adaptation Processes in Insect Olfactory Receptors. Annals of the New York Academy of Sciences. 1987;510:104–112. doi:10.1111/j.1749-6632.1987.tb43475.x.

[74] Brandão SC, Silies M, Martelli C. Adaptive temporal processing of odor stimuli. Cell Tissue Res. 2021;383(1):125–141. doi:10.1007/s00441-020-03400-9.

[75] Jacob V, Monsempès C, Rospars JP, Masson JB, Lucas P. Olfactory coding in the turbulent realm. PLoS Comput Biol. 2017;13(12):e1005870. doi:10.1371/journal.pcbi.1005870.

[76] Lundstrom BN, Hong S, Higgs MH, Fairhall AL. Two Computational Regimes of a Single-Compartment Neuron Separated by a Planar Boundary in Conductance Space. Neural Comput. 2008;20(5):1239–1260. doi:10.1162/neco.2007.05-07-536.

[77] Kadala A, Charreton M, Jakob I, Le Conte Y, Collet C. A use-dependent sodium current modification induced by type I pyrethroid insecticides in honeybee antennal olfactory receptor neurons. Neurotoxicology. 2011;32(3):320–330. doi:10.1016/j.neuro.2011.02.007.

[78] Belmabrouk H, Nowotny T, Rospars JP, Martinez D. Interaction of cellular and network mechanisms for efficient pheromone coding in moths. Proc Natl Acad Sci USA. 2011;108(49). doi:10.1073/pnas.1112367108.

[79] Rapp H, Nawrot MP. A spiking neural program for sensorimotor control during foraging in flying insects. Proc Natl Acad Sci USA. 2020;117(45):28412–28421. doi:10.1073/pnas.2009821117.

[80] Betkiewicz R, Lindner B, Nawrot MP. Circuit and Cellular Mechanisms Facilitate the Transformation from Dense to Sparse Coding in the Insect Olfactory System. eNeuro. 2020;7(2):0305–18. doi:10.1523/ENEURO.0305-18.2020.

[81] Bird AD, Richardson MJE. Transmission of temporally correlated spike trains through synapses with short-term depression. PLoS Comp Biol. 2018;14(6):e1006232. doi:10.1371/journal.pcbi.1006232.

[82] Brown EN, Barbieri R, Ventura V, Kass RE, Frank LM. The Time-Rescaling Theorem and Its Application to Neural Spike Train Data Analysis. Neural Comput. 2002;14(2):325–346. doi:10.1162/08997660252741149.

[83] Barbieri R, Quirk MC, Frank LM, Wilson MA, Brown EN. Construction and analysis of non-Poisson stimulus-response models of neural spiking activity. J, Neurosci Methods. 2001;105(1):25–37. doi:10.1016/S0165-0270(00)00344-7.

[84] Barbieri R, Frank LM, Quirk MC, Wilson MA, Brown EN. Diagnostic methods for statistical models of place cell spiking activity. Neurocomputing. 2001;38-40:1087–1093. doi:10.1016/S0925-2312(01)00450-7.

[85] Fukai T. Computational models of Idling brain activity for memory processing. Neurosci Res. 2022;doi:10.1016/j.neures.2022.12.024.

[86] Pézier A, Acquistapace A, Renou M, Rospars JP, Lucas P. Ca2+ Stabilizes the Membrane Potential of Moth Olfactory Receptor Neurons at Rest and Is Essential for Their Fast Repolarization. Chem Senses. 2007;32(4). doi:10.1093/chemse/bjl059.

[87] Hallem EA, Ho MG, Carlson JR. The Molecular Basis of Odor Coding in the Drosophila Antenna. Cell. 2004;117(7):965–979. doi:10.1016/j.cell.2004.05.012.

[88] Malnic B, Hirono J, Sato T, Buck LB. Combinatorial Receptor Codes for Odors. Cell. 1999;96(5):713–723. doi:10.1016/S0092-8674(00)80581-4.

[89] Cao LH, Yang D, Wu W, Zeng X, Jing BY, Li MT, et al. Odor-evoked inhibition of olfactory sensory neurons drives olfactory perception in Drosophila. Nat Commun. 2017;8(1):1357. doi:10.1038/s41467-017-01185-0.

[90] Levakova M, Kostal L, Monsempès C, Lucas P, Kobayashi R. Adaptive integrate-and-fire model reproduces the dynamics of olfactory receptor neuron responses in a moth. J R Soc Interface. 2019;16(157):20190246. doi:10.1098/rsif.2019.0246.

[91] Stevens CF. A statistical property of fly odor responses is conserved across odors. Proc Natl Acad Sci USA. 2016;113(24):6737–6742. doi:10.1073/pnas.1606339113.

[92] Olsen SR, Bhandawat V, Wilson RI. Divisive Normalization in Olfactory Population Codes. Neuron. 2010;66(2):287–299. doi:10.1016/j.neuron.2010.04.009.

[93] Levakova M, Kostal L, Monsempès C, Jacob V, Lucas P. Moth olfactory receptor neurons adjust their encoding efficiency to temporal statistics of pheromone fluctuations. PLoS Comput Biol. 2018;14(11):e1006586. doi:10.1371/journal.pcbi.1006586.

[94] Voges N, Chaffiol A, Lucas P, Martinez D. Reactive Searching and Infotaxis in Odor Source Localization. PLoS Comput Biol. 2014;10(10):e1003861. doi:10.1371/journal.pcbi.1003861.

[95] Liberzon A, Harrington K, Daniel N, Gurka R, Harari A, Zilman G. Moth-inspired navigation algorithm in a turbulent odor plume from a pulsating source. PLoS One. 2018;13(6):e0198422. doi:10.1371/journal.pone.0198422.

[96] Jayaram V, Kadakia N, Emonet T. Sensing complementary temporal features of odor signals enhances navigation of diverse turbulent plumes. eLife. 2022;11. doi:10.7554/eLife.72415.

[97] Kadakia N, Demir M, Michaelis BT, DeAngelis BD, Reidenbach MA, Clark DA, et al. Odour motion sensing enhances navigation of complex plumes. Nature. 2022;611(7937):754–761. doi:10.1038/s41586-022-05423-4.

List of attachments

Attachment I Manuscript published in *Physical Review E* **103**, 022408. Published on 18th February 2021, IF 2.707
doi: https://doi.org/10.1103/PhysRevE.103.022408

Attachment II Unpublished report

Attachment III Manuscript published in *PLoS Computational Biology* **103**, 022408. Published on 2nd December 2019, IF 4.779
doi: https://doi.org/10.1371/journal.pcbi.1007545

Attachment IV Manuscript published on *bioRxiv*.
Published on 15th March 2023
doi: https://doi.org/10.1101/2023.03.13.532471

Attachment V Manuscript published on *bioRxiv*.
Published on 22nd July 2022
doi: https://doi.org/10.1101/2022.07.21.501055

Attachment VI Unpublished report